Total cross-section measurements for positrons and electrons scattered by sodium and potassium atoms

C. K. Kwan, W. E. Kauppila, R. A. Lukaszew, S. P. Parikh, T. S. Stein, Y. J. Wan,* and M. S. Dababneh†

Department of Physics and Astronomy, Wayne State University, Detroit, Michigan 48202

(Received 7 June 1990; revised manuscript received 19 December 1990)

Absolute total-scattering cross sections (Q_T's) have been measured for positrons and electrons colliding with sodium and potassium in the 3–102-eV range, using the same apparatus and experimental approach (a beam-transmission technique) for both projectiles. Comparing the present measured Q_T's for positron and electron scattering by each separate alkali-metal atom shows that (1) they are very similar in shape and magnitude over the entire energy range investigated, (2) they tend to merge near (and above) the relatively low energy of about 40 eV, and (3) the positron Q_T's become higher than the corresponding electron values as the projectile energy is decreased below about 40 eV. These positron and electron Q_T comparison measurements differ markedly from the situation for room-temperature gases, but are supported by recent theoretical calculations both for the positron and electron Q_T comparisons and for their respective absolute values.

I. INTRODUCTION

One of the main incentives for making direct comparison measurements between positron and electron scattering from the same target gases is the potential that such comparisons have for providing deeper insight into atomic-scattering phenomena than may be acquired by studying the scattering of only one type of projectile from various gases. As an example, direct comparison measurements of positron and electron total-scattering cross sections (Q_T's) have shown that the electron-He Q_T's are considerably larger than the corresponding positron values at low energies [1] (about a factor of 100 in the vicinity of 2 eV), but tend to be merged [2] (to within 2%) near and above the relatively low energy of 200 eV. Although, prior to these measurements, it had been expected that positron- and electron-atom (molecule) cross sections would merge at sufficiently high energies (where the first-Born approximation is valid), distorted-wave second-Born-approximation (DWSBA) calculations [3], considered to be among the most reliable calculations available for the positron- and electron-He collision system, indicate that a merging to the degree observed near 200 eV in the direct positron-electron comparison Q_T measurements by Kauppila *et al.* [2] would not be expected to occur until about 2000 eV. Furthermore, in the vicinity of 200 eV, where the merging of positron and electron Q_T's has been observed to occur, the DWSBA calculations [3] predict that the total (integrated) elastic-scattering cross section for electrons is more than twice as large as the corresponding positron integrated elastic cross section. One of the intriguing questions suggested by the helium investigations referred to above [2,3] is how the Q_T's for positrons and electrons can merge in the vicinity of 200 eV, where the partial contributions (such as the integrated elastic cross section Q_E) to Q_T appear to still be behaving much differently. Is it merely an accident in the case of helium that Q_E for electrons is much larger than the corresponding cross section for positrons, and the combined inelastic-scattering cross sections for positrons are just the right amount larger than the corresponding cross sections for electrons, so that the corresponding Q_T's are merged near and above 200 eV? A related question is, what is responsible for the merging of the corresponding positron and electron Q_T's at energies far below the expected asymptotic energies at which the first-Born approximation is valid? These questions have been addressed in articles by Walters [4] and by Byron, Joachain, and Potvliege [5], and will be discussed further in Sec. IV of this article, because they may also have a bearing upon the interpretation of the present positron- and electron-Na and -K Q_T measurements.

The general tendencies described above for the positron- and electron-He Q_T comparison measurements appear in nearly all of the existing direct comparison measurements of Q_T's for room-temperature gases [6]. At low energies, there is a tendency for the electron Q_T's to be substantially larger than the corresponding positron Q_T's (except in the immediate vicinities of particularly deep Ramsauer-Townsend minima which occur for electrons colliding with certain gases, such as Ar, Kr, and Xe) [6]. As the projectile energy is increased to sufficiently high values, there is a tendency for the positron and electron Q_T's to approach each other. Mergings (within the uncertainties of the respective measurements) of positron and electron Q_T's have actually been observed for helium [2] (as mentioned above), molecular hydrogen [7], and water vapor [8] in the vicinity of 200 eV.

Part of our motivation for our initial investigations [9] of the alkali-metal atoms was due to our being curious about whether all atoms and molecules exhibit the same general trends for positron- and electron-scattering comparisons as those described above. Compared with room-temperature gases, the alkali-metal atoms have rel-

atively low electronic excitation thresholds (e.g., 2.10 eV for Na and 1.61 eV for K) and large polarizabilities [10]. In addition, since the alkali-metal atoms all have ionization threshold energies less than the binding energy (6.8 eV) of positronium (Ps) in its ground state, Ps can be formed by positrons of arbitrarily small incident energy, and so the Ps formation channel is always open for these atoms in contrast to the situation for the room-temperature gases [6].

Our first report on the measurement of positron– and electron–alkali-metal-atom Q_T's was on potassium [9], where we found that the corresponding positron and electron Q_T's were much closer to each other over the entire energy range studied (5–49 eV) than had been observed for any other target atoms and molecules investigated previously. Since then we have improved our method (described in Sec. III) of measuring the scattering cell temperature which is used to determine the atom number density in that cell, and using this improved method, we have remeasured positron- and electron-K Q_T's, extended the energy range of the original measurements [9], and measured positron- and electron-Na Q_T's. In this paper, we present absolute Q_T's measured for positrons and electrons colliding with sodium and potassium in the 3–102-eV energy range. The present positron-Na results represent Q_T measurements for this collision system, which to the authors' knowledge have not been reported previously. We regard the present positron- and electron-K and electron-Na results as superseding our earlier measurements on these collision systems [9,11].

II. EXPERIMENTAL APPARATUS

The experimental apparatus used in the present measurements is essentially the same as that used in our initial measurements on potassium [9], except for some changes (described below) in the way that we measure the temperature of our scattering cell. The apparatus incorporates a major part of the system [1,2,12] which we have used for measuring Q_T's for room-temperature gases. The positron source is ^{11}C, produced on site by the $^{11}B(p,n)^{11}C$ reaction which is generated by bombarding an elemental boron target with 4.0–4.5-MeV protons from a Van de Graaff accelerator. The positrons which are detected have a measured energy width [13] (full width at half maximum) of less than 0.10 eV. In order to make direct comparisons between the scattering of positrons and electrons in the same apparatus, the positron source can be replaced by an electron source (type-B Philips cathode) mounted in the same location and having a similar geometry to that of the positron source. The measured energy width of the detected electron beam is in the range of 0.15–0.20 eV. A curved solenoid (45° bend; radius of curvature, 91.4 cm), which served as the scattering region for our room-temperature gas Q_T measurements [12], is used in the present alkali-metal-atom Q_T measurements mainly to help guide the projectile beam over the approximate 1.3-m-long distance from the source to the alkali-metal-atom scattering cell, and to discriminate against high-energy particles coming from the positron source.

A schematic diagram of the alkali-metal-atom scattering system is shown in Fig. 1. The major component in this region is the vaporization oven (made of type-304 stainless steel) which includes the scattering cell and a detachable cylinder which is loaded with the alkali metal to be studied. The scattering cell is a hollow rectangular block with short cylindrical channels leading to circular knife-edged apertures at each end of the oven (entrance and exit aperture diameters are 3.18 and 3.57 mm, respectively). The detachable cylinder, which is screwed on to the main oven body, is knife edged (to reduce "creeping" of alkali metal out of its reservoir) and has a ground-flat surface where it seals against the main oven body (to prevent leakage of alkali metal from that joint). The cylinder is also copper clad to reduce temperature variation over its length. Bifilar heating elements (tantalum wire in four-holed alumina insulators) are located in the walls of the main oven body and in the part of the outer copper lining which is at the bottom of the detachable cylinder. There are no detectable effects (due to stray magnetic fields) on the projectile beam when the heater currents are switched on and off or when the direction of the heater current is reversed. The heater elements are located closer together near the entrance and exit apertures to maintain the aperture plates at a slightly higher temperature than the remainder of the oven in order to reduce their tendency to become clogged by condensation of alkali metals. The vaporization oven is held in place by five adjustable type-304 stainless-steel screws which are sharpened to points in order to minimize the transfer of heat from the oven to its surroundings.

During actual experimental runs, temperatures in the vaporization oven are monitored in three locations in the

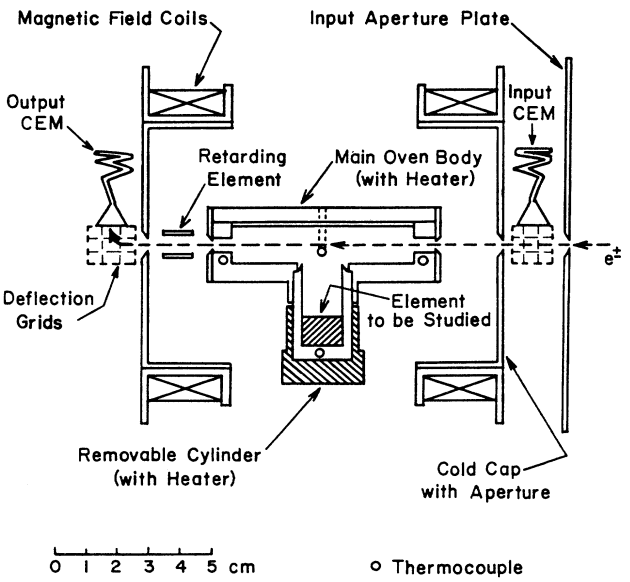

FIG. 1. Schematic diagram of the alkali-metal atom scattering system.

walls of that oven: near the bottom of both of the oven's side walls and in the bottom of the detachable cylinder as shown in Fig. 1. The oven temperatures are measured using chromel-alumel thermocouples (electrically insulated by alumina tubes) inserted in cylindrical channels in the oven walls and in the bottom of the detachable cylinder. There are also channels for inserting thermocouples near the apertures of the oven (as shown in Fig. 1).

Relatively simple changes in the way that we monitor the scattering cell temperature have significantly improved the reproducibility and accuracy of our temperature measurements compared to those in our original alkali-metal Q_T experiment [9]. In order to avoid changes in the positions of the thermocouples over long periods of time (which could affect Q_T comparisons between positrons and electrons as well as the measured absolute Q_T values for either projectile), they are inserted in their respective channels until they touch the closed ends of those channels, and are then secured in place by set screws which contact the alumina insulators. To reduce heat transfer from the thermocouple junctions to the environment outside of the oven, very thin (0.127 mm diameter) thermocouple wire is used, and the alumina insulators are broken into several pieces along their length. The thermocouple wire used in our original alkali-metal Q_T measurements [9] had a 0.254 mm diameter and the thermocouple insulating tubes were left intact.

The weak guiding axial magnetic field produced by the curved solenoid is extended into the scattering region by means of two coils located concentrically with the entrance and exit apertures of the scattering cell. A Channeltron electron multiplier (CEM) on the input side of the oven with its cone (front end) biased at an attractive potential, is used to measure the incident beam intensity. When the cone of that detector is placed at ground potential, the projectile beam is permitted to pass through the oven and the transmitted beam is detected by another CEM at the output end of the oven. Beam detection efficiency is enhanced by using a pair of biased vertical stainless-steel (type-304) grids near each CEM. Whenever the projectile energy is set at a new value, the voltages on these grids are adjusted so as to produce an appropriate transverse electric field in the vicinity of each CEM which together with the axial magnetic field from the solenoids provide an $\mathbf{E}\times\mathbf{B}$ drift toward the cone of each CEM. A stainless-steel (type-304) cylindrical retarding element located between the oven and the output CEM is used to measure the projectile energy as well as to provide additional discrimination (discussed in Sec. III) beyond geometrical considerations, against projectiles scattered through small angles in forward directions. Water-cooled copper end caps which surround the entrance and exit apertures of the oven serve to minimize the transfer of alkali metal from the oven to other parts of the scattering region (with the exception of the retarding element referred to above which is deliberately exposed to the effusing vapor for reasons discussed in Sec. III D). The location of the CEM's off of, and transverse to the projectile beam axis and behind the copper end caps, reduces their exposure to the alkali-metal vapor which is effusing from the oven.

III. EXPERIMENTAL PROCEDURE AND ERROR ANALYSIS

In an ideal beam-transmission experiment, the total-scattering cross section (Q_T) can be obtained from the relationship

$$I=I_0e^{-nLQ_T} \tag{1}$$

by measuring the projectile beam current (I_0) transmitted through an evacuated scattering cell of length L, and the projectile beam current (I) transmitted through the same scattering cell when it contains gas (or vapor) of number density n. In our alkali-metal-atom experiment, the alkali-metal vapor is cycled in and out of the scattering cell by alternately heating the oven, and then letting it cool. The duration of a single Q_T measurement is typically a few hours due mainly to the amount of time required to heat the oven, let it come to thermal equilibrium so that beam-transmission measurements can be made with appreciable alkali-metal vapor in the oven, and then letting the oven cool sufficiently that there is negligible vapor in it. Over such long periods of time, the incident projectile beam intensity varies too much (especially in the positron case, due to the 20 min half-life of ^{11}C) to simply compare the transmitted beam intensity with a significant amount of vapor in the oven to the transmitted beam intensity with negligible vapor in the oven. The use of an input CEM and an output CEM as described in Sec. II enables us to normalize the transmitted beam intensity with respect to the varying incident beam intensity.

Our Q_T's are determined by measuring (1) the ratio R_{cold} of the output CEM to the input CEM counts per second when the oven is relatively cool so that there is a negligible vapor pressure in the oven, and (2) the ratio R_{hot} of the output CEM to the input CEM counts per second with the oven at an elevated temperature so that there is a high enough vapor pressure in the oven to attenuate the projectile beam appreciably. Determinations of $R_{\text{hot}}/R_{\text{cold}}$, n, and L are used with the relationship

$$R_{\text{hot}}=(R_{\text{cold}})e^{-nLQ_T} \tag{2}$$

to obtain absolute positron– and electron–alkali-metal-atom Q_T's.

A. Determination of atom number density n

We obtain the atom number density in our oven by measuring the temperature T of the oven and then obtaining the corresponding equilibrium vapor pressure P from published vapor-pressure data [14]. The atom number density is obtained from the ideal-gas expression,

$$n=P/kT\ . \tag{3}$$

(Use of the ideal-gas expression [Eq. (3)] is justified in our experiment, since the vapor pressure is of the order of only 10^{-4} to 10^{-3} Torr.) There is potential for substantial errors in the determination of n by the procedure described above due mainly to the following reasons. The vapor pressures of sodium and potassium depend very

sensitively on the temperatures of these metals. For instance, in the range of temperatures where we have made our measurements (225–249 °C for Na and 138–156 °C for K) an increase in the temperature of just 10 °C increases the vapor pressure of Na by a factor of about 1.6 and the vapor pressure of K by a factor of about 1.8. In addition, the published vapor-pressure data that we use can itself have substantial uncertainties [14]. According to Eq. (2), an uncertainty Δn in the determination of n would result in an uncertainty ΔQ_T in the measured cross section Q_T given by

$$\Delta Q_T / Q_T = \Delta n / n \ . \tag{4}$$

From Eq. (3) it can be seen that the uncertainty in the number density, Δn, is related to the respective uncertainties in the vapor pressure, ΔP, and in the oven temperature, ΔT. However, the uncertainties in the vapor pressure and oven temperature are not independent of each other because, as mentioned above, we use the oven temperature to determine the vapor pressure. A discussion of the uncertainty in n related to these considerations, and of the steps that we have taken to minimize the error in n, is provided below.

In order to try to achieve the equilibrium vapor pressure in our oven which actually corresponds to a given average oven temperature, we always try to coat the insides of the oven walls with alkali-metal droplets before making the actual Q_T measurements by heating the alkali-metal-containing cylinder to a higher (by about 10 °C) temperature than the transmission cavity for a prolonged period of time (about 3 h). When the oven has been opened up for periodic cleaning, there have been clear visual indications that a coating is present over very nearly the entire inner oven surface, if not the entire surface. The oven temperature is determined by taking the average of the readings of the two thermocouples embedded in the side walls of the oven and the thermocouple embedded in the bottom of the cylinder which contains the alkali metal. In the discussion which follows, these three readings, as a group, will be referred to as the "wall-temperature readings." The thermocouples are each periodically calibrated using an ice-water mixture and boiling water, and are only used if they read within 0.2 °C of the correct temperature values at these calibration points. During actual Q_T measurements, the spread of the three wall-temperature readings and the drift of each of the readings are monitored throughout each run. For all of the data used in this article, the maximum deviation between each of the measured wall temperatures and the average of those temperatures over the duration of any Q_T measurement for a given energy was less than 1.5 °C.

As an additional check on the accuracy of the oven temperature measurements, a fourth thermocouple has been suspended in the interior of the oven's cavity with and without appreciable alkali-metal vapor in the oven. It has been inserted through the entrance aperture of the oven and it is supported in such a way that it is not in direct contact with any part of the interior surface of the oven, and also in such a way that heat transfer along the thermocouple to the environment outside the oven should be minimized. It has been placed in two different positions, one near the center of the oven, and the other close to one of the apertures (about 1.3 cm from the aperture) in order to determine whether the temperature of the cavity interior where the projectile beam travels is the same as the average of the wall-temperature readings. The difference between the cavity-interior temperature readings and the average of the wall-temperature readings is less than 1 °C over the entire range of temperatures used in the present experiments (from 138 to 249 °C). Due to practical considerations, the fourth thermocouple is removed during actual Q_T measurements.

Based upon the tests and calibrations we have made of our oven temperature measurements, we feel that it is reasonable to assign an uncertainty to those measurements of ±2.5 °C in the 225–249 °C temperature range for Na and ±1.5 °C in the 138–156 °C temperature range for K. This consideration, by itself, translates into a ±12% uncertainty in the vapor pressure for Na and a ±9% uncertainty in the vapor pressure for K.

Honig and Kramer [14] have mentioned that it is rare to have the accuracy of vapor-pressure measurements better than ±20% of the reported values. Although some recent measurements of vapor pressures [15,16] have been reported with uncertainties of just a few percent, the magnitudes of the differences between some relatively recent corresponding measurements made by different groups suggest that one should be wary of selecting vapor-pressure data solely on the basis of the small size of the reported uncertainties of the measurements. As just one example which is relevant to the present Q_T experiments, measurements of sodium-vapor density by Ioli, Strumia, and Moretti [15] using an optical (atomic absorption) method in the temperature range from 100 to 180 °C, indicate that the vapor pressure of Na at a temperature of 238 °C would be 9.0×10^{-4} Torr with a reported error of less than 3%, including systematic errors. In contrast to this result, measurements of Na-vapor densities using a laser resonance fluorescence method by Fairbank, Hansch, and Schawlow [17] in the temperature range from −28 to 144 °C indicate that the vapor pressure of Na at the same temperature as mentioned above for Ioli, Strumia, and Moretti (238 °C) would be 1.33×10^{-3} Torr, which is nearly 50% larger than the value indicated by the measurements of Ioli, Strumia, and Moretti. Fairbank, Hansch, and Schawlow [17] indicate that the random and systematic errors of their density measurements over the range from 7 to 144 °C are less than 10%, but there is no assessment of the uncertainty for vapor-pressure values obtained from their derived vapor-pressure equations above 144 °C.

Rather than trying to select the vapor-pressure measurements of a particular experimental group for each alkali metal that we investigate, we have chosen to use a compilation of vapor-pressure results of Honig and Kramer [14], who have invested a major effort in an analysis of data obtained by many different groups for many different elements in order to determine reliable vapor pressures. On the basis of our own survey of published vapor-pressure results, we feel that it is reasonable to assign an uncertainty of ±15% to the vapor-pressure values

reported by Honig and Kramer for Na and for K. Adding this 15% in quadrature to the uncertainties in the Na and K vapor pressures (12% and 9%, respectively) that would be introduced by the uncertainties in our oven temperatures discussed above indicates that a ±20% uncertainty should cover the overall uncertainty in the vapor pressures that we use for Na and K with a small margin of safety. According to Eq. (3), the direct contribution of the uncertainty in T (which is less than 0.5%) to the uncertainty in the number density n is sufficiently small that ±20% should also cover the overall uncertainty in n.

Another consideration with regard to the number density is the gas density distribution profile in the oven under the condition of steady effusive flow. Mathur, Field, and Colgate [18] have calculated effusive flow patterns of cylindrical beam scattering chambers with thin apertures, and have introduced a correction factor α to the measured Q_T such that using the notation of Eq. (2),

$$Q_T = \ln(R_{\text{cold}}/R_{\text{hot}})/(\alpha n L) . \quad (5)$$

α is tabulated [18] in the case of a cylindrical scattering chamber as a function of reduced (in terms of the aperture radius) scattering chamber length H and radius R. Assuming that the shape of the oven (a rectangular shape in our apparatus versus a cylindrical chamber in the case that Mathur, Field, and Colgate have analyzed) does not affect to a great extent the relative density distribution along the axis of the oven, one can use the cross-sectional area of our oven to simulate a circular cross section. In this way we obtain for our scattering chamber the reduced parameters $H=39.1$ and $R=4.01$. From the tabulated values of Mathur, Field, and Colgate [18], α should be essentially 1.00 for the reduced parameters given above. We expect that any deviation of α from 1.00 associated with our oven's relatively short cylindrical channels (described in Sec. II) which lead from the interior of the oven to the knife-edged aperture plates, should be covered by the uncertainty (±20%) that we have assigned to the number density in the discussion above.

The concentration of dimers in the scattering cell is sufficiently low that they are not expected to affect our Q_T measurements to any considerable degree. Using thermodynamic data [19] and a standard method of estimating the concentration of dimers [20], we estimate that dimers constitute less than 0.5% of the total number of target particles in the scattering cell at the temperatures used in this experiment.

Measurements of Q_T at several different gas number densities for each projectile energy can provide tests for the existence of certain types of problems, such as the possible use of vapor-pressure data that may not have the correct temperature dependence, errors (of certain types) in the temperature measurements themselves, or making measurements outside of the single-collision regime. For essentially every Q_T determination that we have made, we have varied the atom number density in our oven by varying the oven's temperature, and we have shown some samples of these number density variation tests in Fig. 2. The tests shown in Fig. 2 as well as all of the other number density variation tests that we have done indicate that there is no significant variation in our measured Q_T values when the number density is varied as much as it is practical for us to vary it (by up to a factor of about 3).

B. Beam path length L

The actual path lengths L of projectiles in the scattering cell can be larger than the straight-line distance L_0 between the entrance and exit apertures of the oven due to spiraling of the projectiles in the guiding axial magnetic field that exists in that region. The average magnetic field in the scattering cell is in the range of 15–35 G for all of the Q_T measurements that we have made. We have estimated upper limits on the percent increase $(\Delta L/L_0)$ in the path lengths of projectiles in the scattering cell using a method described in detail by Kauppila *et al.* [12]. Since these values represent upper limits, and since all of these estimated upper limits on the increases in path lengths are less than 3%, we have simply taken the beam path length L appearing in Eq. (2) to be 6.99 cm, the straight-line distance between the entrance and exit apertures of the oven, and we have folded the estimated upper limits on the increases in path length into our total experimental uncertainty values (discussed in Sec. III E) for each energy at which we have measured Q_T's.

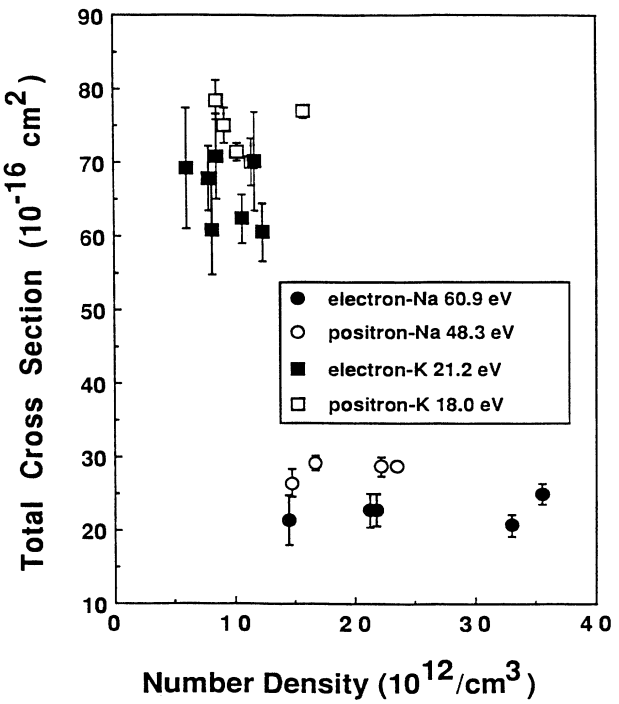

FIG. 2. Measured total cross section vs atomic number density for various projectile-target-energy combinations. The error bars represent the statistical uncertainty for each Q_T value.

C. Discrimination against projectiles scattered through small angles

Experimental and theoretical studies of differential cross sections for electrons scattered by sodium [21–27] and potassium [26–32] have shown that elastic and inelastic scattering are strongly peaked in the forward direction. Theoretical investigations [33–36] indicate that this is also the case for positrons scattered by sodium and potassium. In our experiment, discrimination against projectiles which have undergone small angle scattering is provided by a combination of (1) the size of the oven's exit aperture (3.57 mm diameter) and (2) by the potential applied to the retarding element located between the oven's exit aperture and the output CEM. By setting the retarding potential within 1.25 V (and often within 1.00 V) of the retarding voltage which cuts off the projectile beam when there is negligible alkali-metal vapor in the scattering cell, we are able to achieve essentially 100% discrimination against projectiles which are inelastically scattered by sodium and potassium when there is appreciable alkali-metal vapor in the scattering cell. It is more difficult to discriminate against projectiles which are elastically scattered through small angles in the forward direction, but both of the mechanisms described above (the exit aperture size and the retarding potential) play some role in the angular discrimination against such projectiles. The oven's exit aperture provides discrimination against projectiles which are scattered at sufficiently large angles in the forward hemisphere that the radii of their resulting spiraling motion prohibit their exit from the oven. The angular discrimination due to the size of the scattering cell's exit aperture has been calculated by Kauppila *et al.* [2], and is given by

$$\theta_A = \sin^{-1}[qr_A(B_A B_S/2mE)^{1/2}] , \tag{6}$$

where q is the charge on the electron, m is its mass, r_A is the orbit radius at the exit aperture (which as in Ref. [2] is taken to be $0.65R_A$, where R_A is the exit aperture radius), B_A and B_S are the magnetic fields at the exit aperture and the average magnetic field in the scattering cell, respectively, and E is the projectile energy in the scattering cell.

Discrimination against elastically scattered projectiles by the retarding potential element is provided in the following way. For each projectile energy studied, the potential applied to the retarding potential element is set (with negligible alkali-metal vapor in the scattering cell) so as to decrease the beam intensity to 80% of the beam intensity with no applied retarding potential. As is described by Kauppila *et al.* [12], the steepest portion of the retarding potential curve is at voltages immediately above the retarding potential value that gives 80% beam transmission. When a particle undergoes elastic scattering, some energy associated with axial motion is transferred to energy associated with transverse motion. Since the retarding potential element retards only the axial component of velocity, a particle of incident energy E, which scatters at some angle into the forward hemisphere, may lose sufficient energy associated with axial motion that it will no longer be able to surmount the retarding potential barrier. An estimate by Kauppila *et al.* [2] of the angular discrimination θ_R against elastically scattered projectiles due to the retarding potential has provided the following expression:

$$\theta_R = \sin^{-1}(B_S \Delta E / B_R E)^{1/2} , \tag{7}$$

where B_R is the magnetic field strength at the retarding element and ΔE is the difference of the retarding potential at 40% and 80% of the maximum beam intensity. From Eq. (7) it can be seen that a projectile beam with a narrow energy width (i.e., small ΔE) is essential to obtain a good angular discrimination (small θ_R) by using the retarding potential. The calculation of the axial magnetic fields at various positions of the scattering cell is straightforward, since the magnetic sources are all solenoids of known geometry whose currents are always monitored.

Using Eqs. (6) and (7), the values of the angular discrimination (θ_A and θ_R) provided by the size of the exit aperture and by the retarding potential, respectively, have been determined, and typical values for each energy value at which Q_T's have been measured are shown in Table I. Since the effects of the two angular discrimination mechanisms are independent of one another, the smaller angle represents the upper limit of angular discrimination. It can be seen from the values of θ_A and θ_R in Table I that the retarding element is superior to the size of the exit aperture as a mechanism for providing angular discrimination in our experiment against elastically scattered projectiles, and since θ_R is less than θ_A for all energies at which we have measured Q_T, we take θ_R as the upper limit on the angular discrimination of our apparatus.

The calculated values of discrimination angles given in Table I, along with calculated or measured values of differential elastic cross sections, $\sigma_{el}(\theta,E)$, can be used to estimate the amount ΔQ_T by which our measured Q_T's are low due to incomplete discrimination of our apparatus against small angle elastic scattering, provided that the differential elastic cross sections are known from $\theta=0$ to θ_R. The value of ΔQ_T at a given energy E is given by

$$\Delta Q_T = 2\pi \int_0^{\theta_R} \sigma_{el}(\theta,E)\sin\theta \, d\theta . \tag{8}$$

Recent results for $\sigma_{el}(\theta,E)$ have been used wherever possible for the electron-sodium [21,24,26,27] and electron-potassium [26,27,29,30] estimates of ΔQ_T. Since the integration in Eq. (8) has to be performed from 0°, experimental data have to be extrapolated to the smallest angles. In these cases, we have supplemented the experimental results by the results of Walters [26,27] for the very small angles as has been done by Vuskovic and Srivastava [32] in their determinations of integral cross sections from their differential cross-section measurements. Estimates of ΔQ_T for positrons scattered by Na and K have been made by Ward *et al.* [36] using their five-state close-coupling approximation calculations, and our estimates of angular discrimination. We have included in Table I approximate values of ΔQ_T for positrons scattered by Na and K which we have obtained from re-

TABLE I. Estimated discrimination angles for elastically scattered projectiles deduced for the effects of the exit aperture and for the retarding potential procedure, and estimates of uncertainties in Q_T associated with these angles.

Projectile energy (eV)	Exit aperture θ_A (deg)	Retarding element θ_R (deg)	Estimated ΔQ_T (10^{-16} cm^2)	Estimated $\Delta Q_T/Q_T$ (%)
		Electron-sodium		
4.1	46	14		
5.0			18[a]	20
5.9	33	12		
10.8	23	10		
16.5			7.6[b]	13
20.7	17	8		
30.6			3.1[b]	7
30.7	13	7		
40.8	12	6		
50.8	10	6		
54.4			1.4[b]	5
60.9	8	5		
76.1	7	5		
		Positron-sodium		
2.5			63[c]	40
2.7	58	21		
4.0			35[c]	25
5.0			27[c]	21
7.0			17[c]	16
7.7	37	13		
10.0			8.8[c]	10
17.7	16	10		
20.0			3.7[c]	7
27.7	17	9		
30.0			2.1[c]	5
37.6	15	7		
40.0			1.5[c]	4
48.3	12	7		
50.0			0.9[c]	3
57.9	11	7		
73.3	11	6		
98.3	10	5		
		Electron-potassium		
4.4	39	13		
5.0			28[d]	21
6.2	33	12		
7.0			25[b,e]	22
11.0	22	9		
16.0			11.4[f]	11
21.2	14	7		
30.6			3.0[b]	4
31.3	12	5		
41.4	10	5		
51.4	11	5		
60.0			2.0[e,f]	5
76.8	7	4		
101.9	7	3		

TABLE I. (*Continued*).

Projectile energy (eV)	Exit aperture θ_A (deg)	Retarding element θ_R (deg)	Estimated ΔQ_T (10^{-16} cm^2)	Estimated $\Delta Q_T/Q_T$ (%)
		Positron-potassium		
7.9	34	13		
10.0			19[c]	14
18.0	18	11		
20.0			7.5[c]	9
28.1	15	8		
30.0			3.9[c]	6
38.2	12	8		
40.0			1.9[c]	4
48.2	11	7		
50.0			1.1[c]	2
73.5	9	5		
98.5	9	5		

[a]Reference [21].
[b]References [26] and [27].
[c]Reference [36].
[d]Reference [29].
[e]Reference [32].
[f]Reference [30].

sults presented in figures in the article by Ward *et al.* [36]. In the last column of Table I, we have listed $\Delta Q_T/Q_T$ (as a percent). For electrons, the Q_T's used to obtain $\Delta Q_T/Q_T$ in Table I are taken from the "Walters-Phelps" curves which we introduce and discuss in Sec. IV, while for positrons, the Q_T's are taken from Ward *et al.* [36].

D. Determination of projectile energy

Retarding potential curves are taken for each energy at which we measure Q_T's by monitoring the projectile beam transmitted through the oven and detected by the output CEM as the potential on the retarding element shown in Fig. 1 is varied. A retarding potential curve is taken when the oven is relatively cool (no appreciable alkali-metal vapor in the oven) and when the oven is hot (sufficient alkali-metal vapor in the oven to attenuate the beam appreciably), and finally a third curve is taken when the oven has cooled again. Examples of pairs of "cool-oven" and "hot-oven" retarding potential curves are shown in Fig. 3 for a positron-Na Q_T measurement [Fig. 3(a)] and for an electron-K Q_T measurement [Fig. 3(b)]. Retarding potential curves such as these are used to determine the projectile energy. The inside surfaces of the oven (scattering cell) and of the retarding potential element are coated with the alkali metal being investigated. Since the scattering cell and the retarding element are made of the same material (type-304 stainless steel) it seems reasonable that the effect of alkali-metal deposition would be the same for both. Hence the average energy of the projectiles when they are passing through the scattering cell can be obtained from the retarding potential curve. We assign as the average energy of the incident

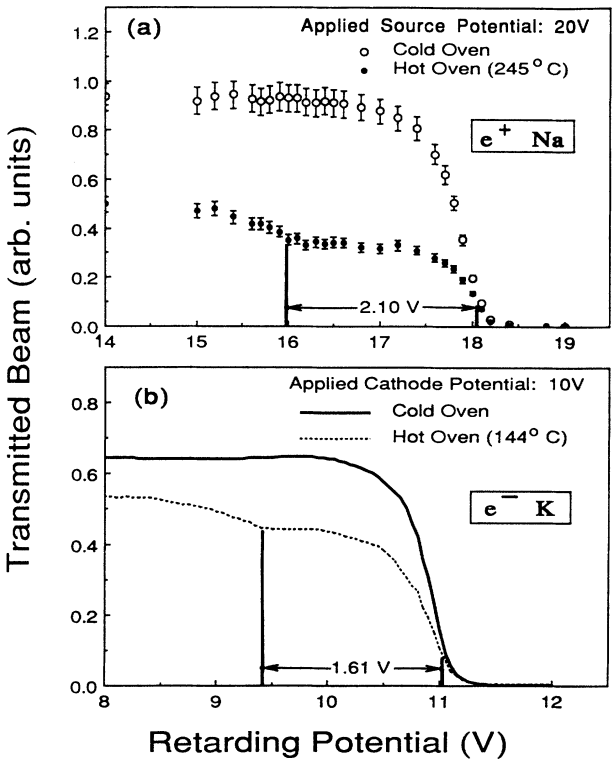

FIG. 3. Retarding potential curves taken with no appreciable alkali-metal vapor in scattering cell (cold oven) and with appreciable alkali-metal vapor in scattering cell (hot oven) for (a) positron-Na case with 20 V applied to positron source; (b) electron-K case with 10 V applied to electron source. All curves shown are taken after the scattering cell and retarding potential element have been coated with the alkali metal being studied.

beam passing through the scattering cell the electronic charge times the retarding voltage that results in a transmitted beam current of approximately 40% of the maximum transmitted current attained just prior to the final steep decline of the retarding potential curve. Based upon our past experience [1,12] with assigning the projectile beam average energy using the retarding potential information, we feel that our assignment of the average energy should be accurate to within several tenths of an eV.

It should be noted that by normalizing currents such as those shown in Fig. 3 to that of the beam entering the oven (detected by the input CEM), we obtain R_{cold} and R_{hot}, and thus have all the beam current information needed to calculate Q_T from Eq. (2), provided that the transmitted currents are taken with the retarding potential set at a sufficiently high value that we have 100% discrimination against projectiles which have undergone inelastic scattering. In practice, for each energy, we calculate Q_T values for three different retarding potentials (which correspond to 80%, 60%, and 40%, respectively, of the maximum transmitted beam intensity with negligible alkali-metal vapor in the oven) and we find that, in general, when there are no noticeable voltage shifts in the retarding potential curves, these all give rise to the same Q_T values within statistical uncertainties. Since a small voltage shift between the "cold" and "hot" curves will give rise to significantly different Q_T's for the 80%, 60%, and 40% retarding potentials, the procedure that we use provides us with a simple check of whether a voltage shift between the hot and cold retarding potential curves occurs.

The possibility that voltage shifts between hot and cold retarding potential curves could affect our measured Q_T values has been recognized since the early stages of our experiment, and care is always exercised to ensure that data are taken in as drift-free a situation as possible. This is accomplished for potassium after coating the oven and the retarding potential element for a few hours. However, in some of the measurements for sodium, we have observed small voltage shifts (of the order of 0.1 V) of the retarding potential curve for the hot run relative to that for the cold run (and even shifts of retarding potential curves corresponding to the cold run made before a hot run relative to the cold run made after the hot run). In such cases, detailed retarding potential curves are taken for a cold oven and for a hot oven, and the hot retarding potential curve is effectively shifted in voltage until it matches (voltagewise) the cold retarding potential curves, and gives rise to the most consistent Q_T's (within the uncertainties of the measurements) for the retarding potential values which give 80%, 60%, and 40% of the maximum transmitted beam current.

An additional observation which can be made in Fig. 3 is that the attenuated (hot-oven) retarding curve has a distinctly different shape (aside from its reduced height) from that of the unattenuated (cold-oven) retarding potential curve. (The cold-oven curves shown in Fig. 3 are actually averages of the retarding curves taken before and after the corresponding hot-oven curves.) The hot-oven curves show noticeable reductions in the transmitted beam currents with cutoffs that correspond to about 2.1 eV lower than the "cutoff energy" of the incident positrons which collide with sodium and about 1.6 eV lower than the "cutoff energy" of the incident electrons which collide with potassium. This and many similar curves which we have taken for positrons and electrons colliding with sodium and potassium provide evidence that the resonance excitations (the $3s$-$3p$ transition for Na and the $4s$-$4p$ transition for K) in these atoms with thresholds at 2.10 and 1.61 eV, respectively, play an important role in the total scattering of positrons and electrons from these atoms, once the projectile energy is several eV or higher. This is known to be the case for electrons colliding with these atoms, but experimental information of this type for positrons has not been available up to the present time.

E. Summary of experimental uncertainties

The uncertainties associated with beam current measurements are essentially statistical and can be readily calculated. Adding in quadrature these statistical uncertainties to the estimated uncertainties in n and L (based on discussions in Secs. III A and III B), we obtain a "total" experimental uncertainty in Q_T of 21% at each projectile energy. This total experimental uncertainty does not include the effect of potential errors arising from incomplete discrimination against projectiles which are scattered elastically through small angles in the forward direction. These are systematic errors which would tend to lower our measured Q_T's, and they are discussed in detail in Sec. III C and summarized in Table I.

It is important to note that the total experimental uncertainty (21%) discussed above applies to our measurements of the absolute Q_T's for positrons and electrons colliding with sodium and potassium. Although the uncertainties associated with these absolute values are of interest, we would like to emphasize that a major thrust of the work described in this article is to make direct comparisons between the Q_T's for positrons and electrons colliding with the same alkali-metal atoms. A significant fraction of the potential errors discussed in this section affect the positron and electron measurements in the same (or at least in a very similar) way and consequently tend to cancel out in a comparison measurement. One of the major potential sources of error which tends to cancel is that due to the determination of the atomic number density n, since very nearly the same oven temperature range is used for the positron and electron measurements for a given alkali metal. Other potential sources of error that tend to affect positrons and electrons in a somewhat similar, but not identical way, are the errors associated with the increases in the path lengths of the projectiles in the scattering cell due to spiraling in the guiding axial magnetic field, and the errors associated with incomplete discrimination against small angle elastic scattering. For the latter effect, cancellation of the errors in the comparison is expected to be incomplete due to (1) differences in the differential elastic-scattering cross sections for the two projectiles, (2) differing relative roles of inelastic versus elastic scattering for positrons compared with electrons, and (3) somewhat different angular discrimina-

tion values for positrons compared with electrons. Even though the cancellation of the latter effects is expected to be incomplete, the tendency toward cancellation will result in a reduction of the overall uncertainties in a comparison of positron and electron scattering from the same target atoms. The error bars on our separate positron and electron results presented in this paper represent the "total" experimental uncertainties (21%) referred to above. The error bars on our positron-electron comparison measurements presented in this paper represent statistical uncertainties, rather than the "total" experimental uncertainties because we feel that statistical uncertainties provide a better indication of the reliability of these comparisons.

IV. RESULTS AND DISCUSSION

Our present positron- and electron-Na and -K absolute Q_T results are listed in Table II. The Q_T value for each energy is the weighted mean of several measurements taken with different oven temperatures. As discussed in Sec. III A, these Q_T values are based upon the vapor-pressure data of Honig and Kramer [14] and a major part of the experimental uncertainty (refer to Sec. III A) associated with our Q_T determinations is due to uncertainty in the published vapor-pressure data that we have used. We have also provided in Table II, along with each Q_T value, the average of the scattering cell temperatures, T_{av}, used for all of our Q_T measurements associated with

TABLE II. Present total cross-section results with statistical uncertainties (in parentheses) for positron- and electron-Na and -K collisions. The total experimental uncertainty in Q_T (discussed in Sec. III E) is 21% at each projectile energy. The oven temperature and vapor pressure (averages obtained from all of the runs which were used to determine each Q_T value) are also provided.

E (eV)	Q_T (10^{-16} cm^2)	T_{av} (°C)	P_V (10^{-4} Torr)
	Electron-sodium		
4.1	67.1 (1.6)	238.4	11.84
5.9	66.5 (2.9)	236.9	11.05
10.8	55.9 (1.2)	239.9	12.65
20.7	43.3 (2.2)	238.3	11.78
30.7	32.6 (2.0)	234.7	9.94
40.8	30.0 (1.7)	238.5	11.90
50.8	26.2 (1.8)	238.5	11.90
60.9	22.9 (0.9)	240.2	12.82
76.1	22.0 (1.1)	236.2	10.70
	Positron-sodium		
2.7	85.8 (1.8)	233.8	9.45
7.7	70.8 (0.5)	232.7	8.92
17.7	52.1 (2.0)	234.1	9.61
27.7	40.8 (0.8)	236.1	10.65
37.6	33.5 (1.2)	236.4	10.80
48.3	28.8 (0.4)	235.0	10.10
57.9	22.0 (0.9)	236.1	10.65
73.3	19.1 (0.7)	234.1	9.61
98.3	18.3 (1.0)	235.0	10.10
	Electron-potassium		
4.4	90.3 (3.6)	141.5	3.24
6.2	89.6 (2.1)	143.8	3.71
11.0	77.7 (1.9)	147.9	4.72
21.2	65.1 (1.9)	145.8	4.16
31.3	51.6 (2.5)	143.4	3.62
41.4	43.9 (1.7)	146.4	4.31
51.4	42.1 (2.7)	148.7	4.94
76.8	37.5 (2.3)	142.8	3.49
101.9	31.5 (1.8)	149.9	5.29
	Positron-potassium		
7.9	106.1 (1.9)	150.2	5.38
18.0	75.7 (1.0)	148.0	4.75
28.1	59.1 (1.0)	149.1	5.05
38.2	47.9 (2.3)	149.0	5.02
48.2	42.1 (1.0)	149.4	5.14
73.5	34.7 (1.5)	148.6	4.91
98.5	30.1 (1.1)	149.2	5.08

each energy and the corresponding vapor-pressure value P_V, obtained from the tabulation of Honig and Kramer [14]. This provides the reader with sufficient information that if the vapor-pressure determinations improve in the future, "corrected" Q_T values, Q_{TC}, can be obtained from the Q_T values listed in Table II by using the improved vapor-pressure values P_{VC} for each value of T_{av} given in Table II, along with the values of P_V which we used, with the approximate relation,

$$Q_{TC}=(P_V/P_{VC})Q_T \ . \tag{9}$$

It should be noted that this is an approximate correction procedure, because when we determine our Q_T values, a value of P_V is determined for each individual Q_T measurement, based on the scattering cell temperature for that measurement. Even so, we feel that the procedure that we have suggested for correcting our Q_T's, if that need should arise, will result in a meaningful correction of those values that can be made in a straightforward way.

A. Electron total cross sections

The present electron-Na and electron-K Q_T measurements are shown in Figs. 4 and 5, respectively, along with the results of prior Q_T measurements [22,32,37,38] and calculations [39–41]. Of the prior measurements, the results of Kasdan, Miller, and Bederson [37], and of Visconti, Slevin, and Rubin [38] (both of these groups using an atom-beam recoil technique) are direct measurements of Q_T's. The results of Srivastava and Vuskovic [22] for Na and of Vuskovic and Srivastava [32] for K are indirect determinations of Q_T's which they obtained by using their own crossed-beam measurements of differential cross sections for elastic scattering and for several different transitions from the ground state, and also excitation and ionization cross sections measured by others. Walters [42] has obtained Q_T's for electron-Na and -K collisions by adding the partial cross sections that he selected from existing theoretical and experimental results for the elastic (Q_E), resonance excitation (Q_R, which represents the $3s$-$3p$ transition for Na and the $4s$-$4p$ transition for K), the sum of the other discrete excitations (Q_D), and the ionization (Q_I) cross sections. Since Walters reported these Q_T values, Q_R and cross sections for numerous other discrete excitations have been measured by Phelps and Lin [43] for Na and by Phelps *et al.* [44] for K, and we have added these more recent excitation cross-section results (rather than the Q_R and Q_D values used by Walters [42]) to the values of Q_E and Q_I selected by Walters, to obtain the Q_T curves shown in Figs. 4 and 5 for Na and K which we will refer to as "Walters-Phelps curves." Our measured electron-Na Q_T values shown in Fig. 4 are similar in shape and slightly

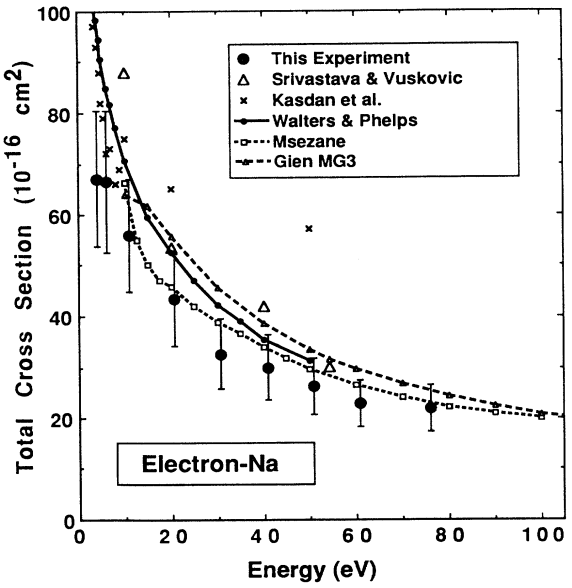

FIG. 4. Electron-Na total cross sections. In this figure and in Figs. 5–7, the error bars represent the "total" experimental uncertainty (discussed in Sec. III E) of the present measurements. The present measurements are compared with the results of prior measurements by Srivastava and Vuskovic (Ref. [22]), and Kasdan, Miller, and Bederson (Ref. [37]); of estimates ("Walters-Phelps" curve based on Refs. [42] and [43] as discussed in Sec. IV A); and of calculations by Msezane (Ref. [39]) and Gien (Ref. [40]), identified in the figure by the respective authors' names. This method of identifying references is used in all of the following figures. The "curves" in this and in the following figures are generated by using straight-line segments to join discrete points taken from the indicated references.

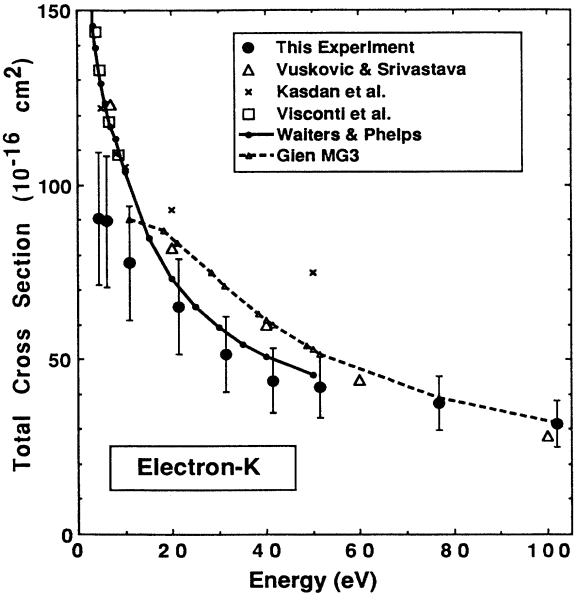

FIG. 5. Electron-K total cross sections. The present measurements are compared with the results of prior measurements by Vuskovic and Srivastava (Ref. [32]), Kasdan, Miller, and Bederson (Ref. [37]), Visconti, Slevin, and Rubin (Ref. [38]); of estimates ("Walters-Phelps" curves based on Refs. [42] and [44] as discussed in Sec. IV A); and of calculations by Gien (Ref. [41]).

lower than the Walters-Phelps curve and are somewhat closer to the theoretical values of Msezane [39] who added the elastic, resonance excitation, 3*s*-3*d*, 3*s*-4*s*, 3*s*-4*p*, and 3*s*-4*d* cross sections obtained from his six-state close-coupling calculation to existing direct ionization cross sections obtained by others. Our measured electron-K Q_T values shown in Fig. 5 are in quite good agreement with the corresponding Walters-Phelps Q_T curve above 20 eV. The electron-Na and -K modified Glauber (MG3) Q_T results of Gien [40,41] shown in Figs. 4 and 5 are somewhat higher than the other theoretical results in those figures. Of the prior Q_T measurements [22,32,37,38], shown in Figs. 4 and 5, the indirect determinations of Srivastava and Vuskovic [22] for Na and of Vuskovic and Srivastava [32] for K are in the closest overall agreement with the present corresponding measurements. The electron-Na and -K Q_T measurements of Kasdan, Miller, and Bederson [37] and the electron-K Q_T measurements of Visconti, Slevin, and Rubin [38] are in quite good agreement with the Walters-Phelps curves near and below 10 eV, but the measurements of Kasdan, Miller, and Bederson for both Na and K diverge from the corresponding Walters-Phelps curves (and from the results of Msezane [39] for Na) above 10 eV, ending up about 80% higher in the case of Na and about 65% higher in the case of K at 50 eV.

As the projectile energy is reduced below 10–20 eV, there is a tendency for our measured electron-Na and -K Q_T's to fall somewhat further below the corresponding Walters-Phelps Q_T curves. Our estimates of errors (given in Table I) introduced into the electron-Na and -K Q_T's due to incomplete discrimination against projectiles elastically scattered through small angles in the forward direction suggest that as the electron energy is reduced below 10–20 eV, the increasing ratio of the elastic scattering cross section (Q_E) to Q_T, and the poorer angular discrimination of our experiment at lower energies may account for our measured Q_T's falling further below the Walters-Phelps curves. At 20 eV and above, on the other hand, we estimate that the amount by which these effects would lower our measured Q_T's would be of the order of 10% or less for electron-Na and -K collisions. Taking into consideration the estimated uncertainties in our measurements and the potential errors in our measured Q_T's associated with the angular discrimination of our measurements, the closeness (and the consistency) of the close-coupling electron-Na Q_T results of Msezane [39] and the Walters-Phelps electron-Na and -K Q_T curves to our own corresponding measured values gives us an indication that our experimental technique and apparatus for measuring absolute electron–alkali-metal-atom Q_T's is basically sound above approximately 20 eV. Since the same apparatus and technique are used for the positron measurements, we feel that they should not be greatly in error above approximately 20 eV.

B. Positron total cross sections

The present measured positron-Na and -K Q_T's are shown in Figs. 6 and 7, respectively, along with prior theoretical results [33,35,36,40,41,45,46]. Ward *et al.*

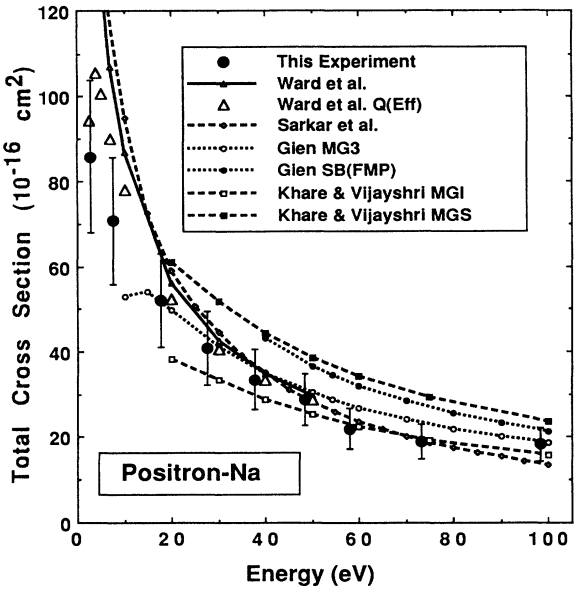

FIG. 6. Positron-Na total cross sections. The present measurements are compared with the results of prior calculations by Ward *et al.* (Ref. [36]), Sarkar, Basu, and Ghosh (Ref. [33]), Gien (Refs. [40] and [46]), and Khare and Vijayshri (Ref. [45]).

[35,36] have performed five-state close-coupling calculations of Q_T for positron-Na and -K collisions that include the cross sections for elastic scattering, resonance excitation, and a few other discrete excitations (3*s*-4*s*, 3*d*, and 4*p* for Na and 4*s*-5*s*, 3*d*, and 5*p* for K) but do not include the cross sections for Ps formation and for ionization which are both expected to be relatively small [42,47]

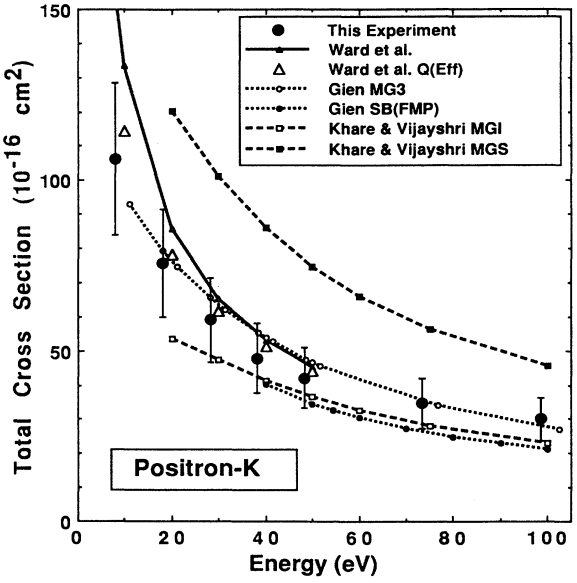

FIG. 7. Positron-K total cross sections. The present measurements are compared with the results of prior calculations by Ward *et al.* (Ref. [36]), Gien (Refs. [41] and [46]), and Khare and Vijayshri (Ref. [45]).

above 10 eV. In addition, Ward *et al.* [35,36] have used our estimates of our angular discrimination (shown in Table I) along with their differential elastic cross-section results to calculate effective cross sections Q_{eff}, which represent their theoretical estimates of the Q_T's that we would be expected to obtain if the only error in our measurements were that associated with the incomplete discrimination of our apparatus against projectiles elastically scattered through small angles in the forward direction. Our measured Q_T's are slightly lower than their corresponding Q_T calculations for Na (Fig. 6) and K (Fig. 7) above 10 eV and are very close to their Q_{eff} values. The positron-Na Q_T results of Ward *et al.* [36] are also quite close to the earlier four-state close-coupling approximation Q_T results of Sarkar, Basu, and Ghosh [33] (Fig. 6) which include their cross sections for elastic scattering, resonance excitation, 3*s*-3*d* and -4*p* excitations, and Ps formation cross sections calculated by Guha and Mandal [47], and first-Born approximation values of ionization cross sections obtained by Walters [42]. The positron-Na and -K modified Glauber approximation ("MG3") Q_T results (Figs. 6 and 7) of Gien [40,41] are also in reasonable agreement with the present results.

Generally speaking, the other positron-Na and -K theoretical Q_T results shown in Figs. 6 and 7 which have not been specifically discussed above are in less satisfactory agreement with the present Q_T measurements. These include the modified Glauber calculations by Khare and Vijayshri [45] based on an "inert core" [MG(IC)] and on the "single particle scattering model" [MG(SPSM)], and the second-Born "full model potential" [SB(FMP)] calculations by Gien [46].

C. Positron and electron total cross-section comparisons

In Figs. 8 and 9, our direct comparison measurements between positron- and electron-Na and -K Q_T's are shown along with selected experimental [43,44] and theoretical [35,36,42,47] results for total, elastic, resonance excitation, the sum of other discrete excitations, ionization, and positronium formation cross sections. We find that Na and K each exhibit remarkably similar Q_T's for positron and electron collisions over the entire energy range that has been studied. We also find that our corresponding positron and electron Q_T's merge within the uncertainties of the measurements in the vicinity of 40 eV and remain essentially merged up to the highest energies studied thus far. In contrast to the case for positron- and electron-room-temperature-gas Q_T's, the positron-Na and -K Q_T's become higher than the corresponding Q_T's for electrons as the projectile energy is reduced from 40 eV down to the lowest energies studied in each case.

The general trends indicated by our positron- and electron-alkali-metal-atom comparisons could be affected somewhat if there were appreciable differences between the errors introduced into the respective Q_T measurements by incomplete discrimination against projectiles elastically scattered through small angles in the forward direction. However, the percent errors ($\Delta Q_T/Q_T$) provided in Table I suggest that although these errors are estimated to be generally slightly larger for electrons than for positrons at corresponding energies, the differences between these errors for the two projectiles are generally too small to significantly alter the general trends indicated by our comparison measurements. In addition, considering that the estimates of $\Delta Q_T/Q_T$ for electrons and positrons are based on different calculations and/or measurements of differential cross sections, the differences between the estimated percent errors shown in Table I for electrons and positrons may not even be significant.

In regard to comparisons of the present Q_T measurements with theoretical results, modified Glauber (MG3) calculations by Gien [40,41] for positron- and electron-Na and -K collisions, shown in Figs. 4–7, predict a different behavior for the positron-electron comparisons than what we have observed. According to Gien's calculations [40,41], the positron- and electron-Na and -K Q_T's do not merge even up to energies as high as 1000

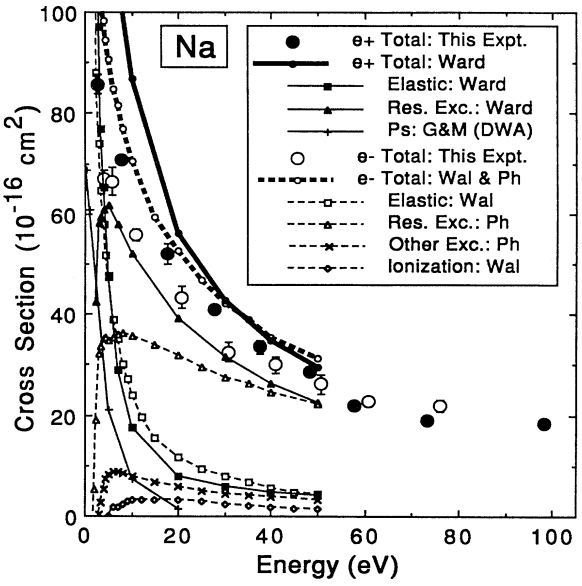

FIG. 8. Comparisons of positron- and electron-Na total and partial cross sections. In this figure and in Fig. 9, the error bars (when larger than the symbol size) represent statistical uncertainties for the present measurements. The present Q_T measurements are compared with the results of a prior Q_T calculation (heavier solid lines) for positrons by Ward *et al.* (Ref. [36]) and estimate (heavier dashed lines) for electrons ("Wal & Ph" refers to the "Walters-Phelps" Q_T curve discussed in Sec. IV A). The partial cross sections (lighter solid lines) shown for positrons are calculations of elastic and resonance excitation cross sections by Ward *et al.* (Ref. [36]) and of positronium formation cross sections ("G&M (DWA)" refers to distorted-wave approximation calculations (with the "post form of the interaction potential") by Guha and Mandal (Ref. [47])). The partial cross sections (lighter dashed lines) shown for electrons are elastic, resonance excitation, the sum of other discrete excitations, and ionization cross sections associated with the "Walters-Phelps" curves described in the text ("Wal" refers to Walters (Ref. [42]) and "Ph" refers to Phelps and Lin (Ref. [43])).

eV, and furthermore, the electron Q_T's are larger than the positron Q_T's over essentially the entire energy range from 10 to 1000 eV, although it should be noted that Gien has not included the effects of exchange in his electron calculations [40,41]. On the other hand, it is interesting that when the Walters-Phelps electron-Na and -K Q_T curves (discussed in Sec. IV A) are compared [48] with the corresponding positron-Na and -K Q_T results obtained by Ward *et al.* [35,36] as shown in Figs. 8 and 9, respectively, mergings, or at least near mergings of the positron and electron Q_T's are observed to occur in the vicinity of 30–50 eV, and as the projectile energy is reduced below this energy range, the positron Q_T's are observed to become increasingly larger than the corresponding electron values for each of these atoms. Thus these comparisons tend to support the general trends that we observe in our positron-electron Q_T comparison measurements.

It is of interest to consider why the present comparisons between positron and electron scattering from Na and K indicate a dominance of the positron over the electron Q_T's at low energies whereas for the room-temperature gases [6], the situation is, for the most part, reversed. Comparisons between positron and electron scattering from the room-temperature gases all seem to fit, in general, a simple interaction model which implies that the positron cross sections at low energies would be expected to be lower than the corresponding electron cross sections due to the tendency toward cancellation of the static and polarization interactions in positron scattering, in contrast to the addition of these interactions in the electron case [6]. Perhaps this simple argument concerning the relative roles of the static and polarization interactions is applicable to the total-scattering cross section if the dominant contribution to it is elastic scattering for both positrons and electrons. However, when inelastic processes become dominant for either positrons or electrons (or both as is the case for Na and K above the relatively low energy of 10 eV as shown in Figs. 8 and 9), this argument in its simple form may no longer apply to a comparison of their total-scattering cross sections. The positron-Na and -K Q_T's may rise above the corresponding electron values as the projectile energy is reduced below 40 eV mainly due to the relatively large contributions to Q_T by inelastic processes, especially excitations, which are predicted to have significantly larger cross sections for positrons [33,35,36] than those that have been measured for electrons [43,44] at these low energies.

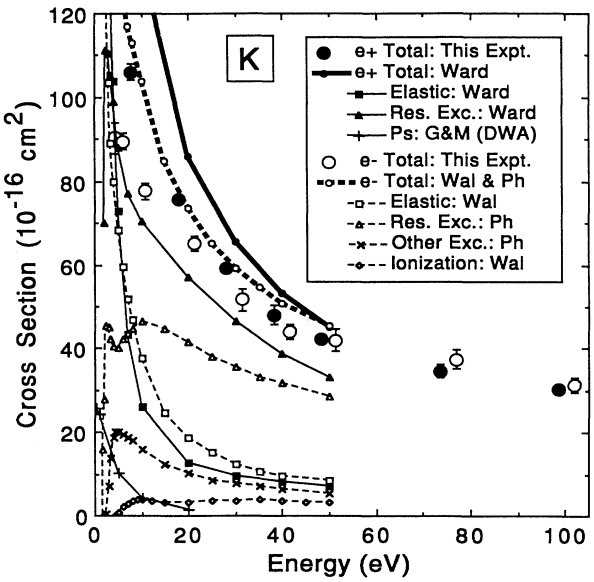

FIG. 9. Comparisons of positron- and electron-K total and partial cross sections. The symbols and curves used to represent the various total and partial cross sections as well as the references associated with those symbols and curves are the same as in Fig. 8, except that "Ph" in Fig. 9 refers to Phelps *et al.* (Ref. [44]).

If our observed low-energy mergings of positron– and electron–alkali-metal-atom Q_T's are valid, this may provide additional evidence that mergings of positron- and electron-atom Q_T's can occur at energies considerably lower than the asymptotic energies at which the first-Born approximation is valid, as is the case for positron- and electron-He collisions referred to in Sec. I. We had commented in Sec. I that near 200 eV, where the positron- and electron-He Q_T's have been observed to merge [2], the partial contributions (such as Q_E) to Q_T are apparently behaving much differently for positrons than for electrons. Evidently, even though the total (integrated) elastic-scattering cross sections for electrons are much larger than the corresponding cross sections for positrons, the sum of the integrated inelastic cross sections for positrons are considerably larger than the corresponding cross sections for electrons, and these opposite behaviors are compensating for each other in such a way that the total-scattering cross sections for both projectiles merge near the relatively low energy of 200 eV (and remained merged at higher energies) [2]. According to recent theoretical calculations [49,50], atomic hydrogen provides another example of this type of behavior. Although our present observations for Na and K indicate that the Q_T's for positrons and electrons may be merging at energies considerably lower than the asymptotic energies at which the first-Born approximation is valid [27], the situation for alkali-metal atoms may be somewhat different than that for helium and atomic hydrogen, since based upon the information in Figs. 8 and 9, the elastic and resonance excitation contributions to Q_T may be at least close to being separately merged where the Q_T's appear to be merging.

In relation to the question of mergings of positron and electron Q_T's at unexpectedly low energies, it is of interest that a theoretical analysis by Dewangan [51] related to higher-order Born amplitudes calculated in the closure approximation has been shown to imply [4,5] that if electron exchange can be ignored in the electron-scattering case, and if the closure approximation is valid, then a merging (or near merging) of positron- and electron-atom Q_T's can occur at energies considerably lower than the asymptotic energies at which the first-

Born approximation is valid.

In light of the information (theoretical and experimental) that we have on positron- and electron-scattering comparisons [6,48] up to the present time, including the present studies of alkali-metal atoms, it is interesting to consider the possibility [48] that at low energies, in general, elastic-scattering cross sections for electron-atom collisions may tend to be larger than those for positron-atom collisions (aside from complications like Ramsauer-Townsend effects), whereas inelastic-scattering cross sections may tend to be larger for positrons than they are for electrons. The tendency toward cancellation of the static and polarization interactions in positron scattering, in contrast to the addition of these interactions in the electron case, may provide a simple explanation for why electron Q_T's could be expected to be larger than the corresponding positron values when elastic scattering is the dominant partial cross section as is the case for the inert gases at low energies [6]. It would be interesting if there could be a correspondingly simple explanation for why inelastic-scattering cross sections may tend to be larger for positrons than for electrons at low energies in general (if this is indeed the case).

ACKNOWLEDGMENTS

We would like to acknowledge Professor H. R. J. Walters for sending us detailed results of his calculations and for very helpful discussions concerning the present work. We are also grateful to Professor J. O. Phelps for sending detailed results of his work, to Professor G. L. Dunifer for the use of his environmental chamber, to Professor G. P. Reck for helpful discussions concerning dimers, and to Dr. G. M. A. Hyder, J. Klemic, and P. J. Keating for assistance in this project. This work was supported by the National Science Foundation under Grant No. PHY87-06120.

*Permanent address: Southeast University, Si Pai Lou *2, Nanjing 210018, People's Republic of China.

†Permanent address: Department of Physics, Yarmouk University, Irbid, Jordan.

[1] T. S. Stein, W. E. Kauppila, V. Pol, J. H. Smart, and G. Jesion, Phys. Rev. A **17**, 1600 (1978).

[2] W. E. Kauppila, T. S. Stein, J. H. Smart, M. S. Dababneh, Y. K. Ho, J. P. Downing, and V. Pol, Phys. Rev. A **24**, 725 (1981).

[3] D. P. Dewangan and H. R. J. Walters, J. Phys. B **10**, 637 (1977).

[4] H. R. J. Walters, Phys. Rep. **116**, 1 (1984).

[5] F. W. Byron, Jr., C. J. Joachain, and R. M. Potvliege, J. Phys. B **15**, 3915 (1982).

[6] W. E. Kauppila and T. S. Stein, Adv. At. Mol. Opt. Phys. **26**, 1 (1990).

[7] K. R. Hoffman, M. S. Dababneh, Y.-F. Hsieh, W. E. Kauppila, V. Pol, J. H. Smart, and T. S. Stein, Phys. Rev. A **25**, 1393 (1982).

[8] O. Sueoka, S. Mori, and Y. Katayama, J. Phys. B **19**, L373 (1986).

[9] T. S. Stein, R. D. Gomez, Y.-F. Hsieh, W. E. Kauppila, C. K. Kwan, and Y. J. Wan, Phys. Rev. Lett. **55**, 488 (1985).

[10] T. M. Miller and B. Bederson, Adv. At. Mol. Phys. **13**, 1 (1977).

[11] T. S. Stein, M. S. Dababneh, W. E. Kauppila, C. K. Kwan, and Y. J. Wan, in *Atomic Physics with Positrons,* Vol. 169 of *NATO Advanced Study Institute, Series B: Physics,* edited by J. W. Humberston and E. A. G. Armour (Plenum, New York, 1987), pp. 251–263.

[12] W. E. Kauppila, T. S. Stein, G. Jesion, M. S. Dababneh, and V. Pol, Rev. Sci. Instrum. **48**, 822 (1977).

[13] T. S. Stein, W. E. Kauppila, and L. O. Roellig, Phys. Lett. **51A**, 327 (1975).

[14] R. E. Honig and D. A. Kramer, RCA Rev. **30**, 285 (1969).

[15] N. Ioli, F. Strumia, and A. Moretti, J. Opt. Soc. Am. **61**, 1251 (1971).

[16] B. Shirinzadeh and C. C. Wang, Appl. Opt. **22**, 3265 (1983).

[17] W. M. Fairbank, Jr., T. W. Hansch, and A. L. Schawlow, J. Opt. Soc. Am. **65**, 199 (1975).

[18] B. P. Mathur, J. E. Field, and S. O. Colgate, Phys. Rev. A **11**, 830 (1975).

[19] M. W. Chase, Jr., C. A. Davies, J. R. Downey, Jr., D. J. Frurip, R. A. McDonald, and A. N. Syverud, J. Phys. Chem. Ref. Data **14**, Suppl. 1, 1412 (1985).

[20] P. W. Atkins, *Physical Chemistry,* 2nd ed. (Freeman, San Francisco, 1982), p. 720.

[21] D. L. Moores and D. W. Norcross, J. Phys. B **5**, 1482 (1972).

[22] S. K. Srivastava and L. Vuskovic, J. Phys. B **13**, 2633 (1980).

[23] B. Jaduszliwer, P. Weiss, A. Tino, and B. Bederson, Phys. Rev. A **30**, 1255 (1984).

[24] J. Mitroy, I. E. McCarthy, and A. T. Stelbovics, J. Phys. B **20**, 4827 (1987).

[25] L. J. Allen, M. J. Brunger, I. E. McCarthy, and P. J. O. Teubner, J. Phys. B **20**, 4861 (1987).

[26] H. R. J. Walters, J. Phys. B **6**, 1003 (1973).

[27] H. R. J. Walters (private communication).

[28] J. A. Slevin, P. J. Visconti, and K. Rubin, Phys. Rev. A **5**, 2065 (1972).

[29] D. L. Moores, J. Phys. B **9**, 1329 (1976).

[30] W. Williams and S. Trajmar, J. Phys. B **10**, 1955 (1977).

[31] S. J. Buckman, C. J. Noble, and P. J. O. Teubner, J. Phys. B **12**, 3077 (1979).

[32] L. Vuskovic and S. K. Srivastava, J. Phys. B **13**, 4849 (1980).

[33] K. P. Sarkar, M. Basu, and A. S. Ghosh, J. Phys. B **21**, 1649 (1988).

[34] G. Ferrante, L. Lo Cascio, and M. Zarcone, Nuovo Cimento Soc. Ital. Fis. B **44**, 99 (1978).

[35] S. J. Ward, M. Horbatsch, R. P. McEachran, and A. D. Stauffer, J. Phys. B **21**, L611 (1988).

[36] S. J. Ward, M. Horbatsch, R. P. McEachran, and A. D. Stauffer, J. Phys. B **22**, 1845 (1989).

[37] A. Kasdan, T. M. Miller, and B. Bederson, Phys. Rev. A **8**, 1562 (1973).
[38] P. J. Visconti, J. A. Slevin, and K. Rubin, Phys. Rev. A **3**, 1310 (1971).
[39] A. Z. Msezane, Phys. Rev. A **37**, 1787 (1988).
[40] T. T. Gien, J. Phys. B **22**, L463 (1989).
[41] T. T. Gien, J. Phys. B **22**, L129 (1989).
[42] H. R. J. Walters, J. Phys. B **9**, 227 (1976).
[43] J. O. Phelps and C. C. Lin, Phys. Rev. A **24**, 1299 (1981); J. O. Phelps (private communication).
[44] J. O. Phelps, J. E. Solomon, D. F. Korff, C. C. Lin, and E. T. P. Lee, Phys. Rev. A **20**, 1418 (1979); J. O. Phelps (private communication).
[45] S. P. Khare and Vijayshri, Indian J. Phys. **61B**, 404 (1987).
[46] T. T. Gien, Phys. Rev. A **35**, 2026 (1987).
[47] S. Guha and P. Mandal, J. Phys. B **13**, 1919 (1980).
[48] T. S. Stein, W. E. Kauppila, C. K. Kwan, R. A. Lukaszew, S. P. Parikh, Y. J. Wan, S. Zhou, and M. S. Dababneh, in *Annihilation in Gases and Galaxies,* NASA Conference Publication 3058, edited by R. J. Drachman (NASA, Washington, DC, 1990), pp. 13–27.
[49] H. R. J. Walters, J. Phys. B **21**, 1893 (1988).
[50] W. L. van Wyngaarden and H. R. J. Walters, J. Phys. B **19**, 929 (1986).
[51] D. P. Dewangan, J. Phys. B **13**, L595 (1980).